

THE EFFECT OF CATHODIC POLARIZATION ON FATIGUE BEHAVIOR

C. E. Jaske
CC Technologies
6141 Avery Road
Dublin, OH 43016-8761 USA

ABSTRACT

The corrosion-fatigue behavior of cathodically protected ASTM A 710, Grade A, Class 3 steel in seawater was studied. The experimental work consisted of fatigue testing of base-metal specimens and weld joints in seawater and the development of a fatigue model. Corrosion-fatigue testing was performed in synthetic seawater at room temperature using sinusoidal loading at a stress ratio of 0.1 and a frequency of 1Hz. Cathodic polarization levels of -0.09 and -1.13V vs. Ag/AgCl were employed. Base-metal specimens had stress-concentration factors of 1.0, 2.0, 3.5, and 5.0 and were subjected to cyclic axial loads. Weld-joint specimens were full-thickness (19-mm) plate that was either butt-welded or fillet-welded; they were subjected to cyclic three-point bending loads. Fatigue crack growth data were developed for the base metal using compact-tension specimens. Both fatigue crack initiation and growth data were developed for the welded joints. Fatigue strength reduction factors were developed to account for the effects of notch severity and weld-joint configuration. A model that uses a fatigue curve to predict crack-initiation life and crack growth rate data to predict crack-propagation life was developed. This model can be employed in structural design.

Keywords: fatigue, cathodic polarization, welded joints, steel, seawater, notch, crack growth

INTRODUCTION

Fatigue is an important potential damage mechanism for structures that operate in marine environments. Examples of marine structures that are subject to fatigue damage include ships, offshore platforms, harbor works, drilling rigs, and underwater pipelines. Fatigue damage is caused by cyclic loadings imposed by winds, waves, tides, and variations in operating conditions. Such loadings, possibly coupled with dynamic amplification, produce

locally high stresses at structural discontinuities such as joints, connections, notches, and welds. Fatigue damage results in the initiation and propagation of cracks at these structural locations. Thus, fatigue damage in marine structures consists of the initiation and growth of cracks at locations of high cyclic stress.

Most marine structures are fabricated from carbon or low-alloy steels. The rate of fatigue crack initiation and growth in such steels can be significantly increased by exposure to seawater. Seawater also causes corrosion of such steels. Cathodic polarization is the most widely used means of protecting submerged marine steel structures from corrosion. Depending on the nature of the seawater environment, the level of polarization, the type of steel, and the fatigue mechanism, cathodic polarization may or may not be an effective means of mitigating fatigue damage. In some situations, cathodic polarization may even aggravate the fatigue damage process. The effect of cathodic polarization on fatigue crack initiation and growth in marine structural steels is an area of practical engineering interest.

Cathodic polarization improves the corrosion-fatigue crack initiation resistance of smooth, uncracked steel specimens tested in seawater. When smooth specimens are tested in seawater under free-corrosion conditions, their fatigue strength is reduced below that of comparable specimens tested in air. The stress versus number-of-cycles-to-failure (S-N) curve for specimens tested in seawater falls well below that of comparable specimens tested in air, especially at low cyclic loading frequencies of 1 Hz or less. Experimental results show that cathodic polarization can improve the fatigue strength of smooth specimens tested in seawater to levels comparable or even slightly above those of smooth specimens tested in air.

For corrosion-fatigue crack initiation at notches, however, cathodic polarization may or may not provide effective protection. Lower levels of polarization provide a degree of benefit, while higher levels of polarization may actually degrade fatigue strength. This behavior is related to the strength and microstructure of the steel and the notch severity. The degradation of fatigue performance at higher levels of polarization is believed to be caused by the effect of hydrogen on the fatigue crack initiation. As notch severity (amount of stress triaxiality at the notch tip) and material strength increase, the susceptibility to hydrogen-induced degradation also increases. Corrosion-fatigue crack initiation at notches, such as weld toes and weld defects, is a significant problem for marine structures, so it is important to understand the effects of cathodic polarization on corrosion-fatigue crack initiation at notches.

Cathodic polarization has mixed effects on corrosion-fatigue crack propagation in seawater. Mild levels of polarization may slightly improve corrosion-fatigue crack-growth resistance, but the levels typically employed in the protection of marine structures often accelerate corrosion-fatigue crack growth because of the detrimental effects of hydrogen generated by the cathodic reaction. When calcareous deposits form within a crack, crack-closure effects that decrease the range of the effective crack-tip stress intensity factor can decrease crack-growth rates. Therefore, cathodic polarization can either increase or decrease the corrosion-fatigue crack propagation rates for steels in seawater.

Seven major variables can affect the interaction of cathodic polarization and corrosion-fatigue of structural steels in seawater:

1. *Cyclic stress range.* High stress ranges cause relatively rapid fatigue damage and crack growth, and the effects of the environment are minimal. Low stress ranges cause fatigue damage to develop slowly, so corrosion has time to accelerate the rate of fatigue-crack initiation. Corrosion often has little effect on the rate of crack propagation at low stress ranges, but it can greatly increase the rate of fatigue crack growth at intermediate stress ranges.
2. *Cyclic frequency.* The lower range of the cyclic loading frequencies to which marine structures are typically exposed (0.1 to 1.0 Hz) can significantly lower fatigue strength and increase crack-growth rates.
3. *Cathodic polarization.* Levels of cathodic polarization sufficient to protect marine structures from corrosion can have either a beneficial or a detrimental effect on fatigue behavior.
4. *Notches and defects.* Notches and defects provide local stress concentrations where fatigue cracking is more likely to initiate and can reduce the effectiveness of cathodic polarization. Notches and defects associated with weld joints are of particular practical importance in marine structures.
5. *Cracks.* It is difficult to protect cracks effectively from the detrimental effects of marine corrosion using cathodic polarization. Furthermore, hydrogen produced by the cathodic reaction often accelerates the fatigue crack growth rate. If calcareous deposits form within a crack, the rate of crack growth is usually decreased because of crack closure.
6. *Alloy composition.* The alloying elements, at the levels that they are typically present in structural steels, have little direct influence on their corrosion-fatigue resistance in seawater. They do, however, indirectly affect fatigue strength through their influence on microstructure and strength level after heat treatment and welding.
7. *Biological species.* Biologically active species can affect corrosion-fatigue of marine structures in two ways. Macrobial growths can increase hydrodynamic loading and, hence, reduce the fatigue performance of the structure. Microbial growths can increase the fatigue-crack-growth rate and decrease fatigue strength. This behavior is caused by the presence of small amounts of H₂S in the seawater. The H₂S is a metabolic product of sulfate-reducing bacteria.

All of these seven factors were reviewed in detail and evaluated in developing the plans for this research.¹ Tests were performed at several different stress levels, three levels of cathodic polarization, and three degrees of notch severity. A reasonable cyclic frequency of 1 Hz was employed for all fatigue testing in seawater. Both crack-initiation and crack-growth behavior were evaluated. ASTM A 710, Grade A, Class 3 steel plate was selected for the fatigue testing

because it is representative of typical modern, high-strength low-alloy steels used for marine applications. The effects of biologically active species on corrosion fatigue were outside of the scope of the work, so all corrosion-fatigue tests were conducted in synthetic seawater. Thus, the main factors expected to influence the corrosion-fatigue behavior of cathodically polarized steel in seawater were addressed in this research.

The objectives of the research were (1) to investigate the effect of cathodic polarization on fatigue of steel in seawater and evaluate how this effect is influenced by notch severity, crack size, and material composition, microstructure, and strength and (2) to formulate a model to predict how the fatigue properties of steel in seawater are influenced by cathodic polarization.

TECHNICAL APPROACH

The research work was divided into the following four tasks: (1) comprehensive literature review, (2) fatigue experiments in seawater, (3) fatigue of welded specimens in seawater, and (4) development of a fatigue model. The literature review extended a previous extensive review of publications on corrosion fatigue of steels in marine environments.² Results of the literature review were used to finalize the plans for the fatigue testing and to help develop the fatigue model.

Scope of Work

Published literature on electrochemical potential and fatigue interactions for steels in seawater was comprehensively searched, concentrating on documents published since 1981 or after the review of Jaske, et al.² The search utilized the resources of technical libraries at Battelle and The Ohio State University in Columbus, Ohio. The 296 documents obtained from this comprehensive literature search were thoroughly reviewed, evaluated, and used to compile a detailed bibliography.¹

Corrosion-fatigue experiments on specimens from ASTM A 710, Grade A, Class 3 steel plate were performed in ASTM synthetic seawater. The fatigue specimens were subjected to sinusoidal loading at a stress ratio (R) of 0.1. R is the ratio of minimum to maximum cyclic stress. A few fatigue tests were conducted in air to develop baseline fatigue data. A cyclic frequency of 10 Hz was used for the tests in air, whereas a cyclic frequency of 1 Hz was used for the tests in seawater. S-N curves were developed for both smooth and notched specimens of base metal. Fatigue crack growth data also were developed for base metal. Both S-N curves based on crack initiation and fatigue crack growth data were developed for butt-welded and fillet-welded specimens with varying degrees of notch severity at the weld toes. Both typical (-0.90 V vs. Ag/AgCl) and high (-1.13 V vs. Ag/AgCl) levels of cathodic polarization were used in the experiments. The results of these tests characterized the corrosion-fatigue behavior of cathodically polarized base metal and weldments in seawater.

Based on the experimental data and information collected from the literature, a model was developed to predict the influence cathodic polarization on the fatigue behavior of the steel in seawater. The model incorporates the effects of cathodic polarization on both fatigue crack initiation and propagation, while taking into account the effect of notch severity on crack

initiation and the effect of calcareous deposits on crack growth. It is formulated in terms of straightforward equations, so it can be implemented easily by marine engineers and incorporated into computer codes used for the fatigue assessment of marine structures.

Material

Three pieces from a 19-mm (3/4-inch) thick plate of ASTM A 710, Grade A, Class 3 steel were obtained. Each piece was approximately 0.61 by 0.61 m (24 by 24 inches). The chemical composition and tensile properties of the plate are listed in Tables 1 and 2, respectively. These satisfy the requirements of the ASTM specification, as indicated. This material is a low-carbon age-hardened nickel-copper-chromium-molybdenum-niobium steel that was quenched and precipitation heat-treated. The steel has a combination of reasonably high tensile strength and high toughness, making it ideal for demanding structural applications.

FATIGUE EXPERIMENTS IN SEAWATER

Fatigue experiments were performed on axially loaded smooth (unnotched) and notched base-metal specimens to develop stress versus number-of-cycles-to-failure (S-N) curves. Fatigue crack growth experiments were performed on base-metal compact-tension (CT) specimens to develop cyclic crack growth rate (da/dN) data as a function of the range of the applied stress intensity factor (ΔK).

S-N Fatigue

Four types of base-metal fatigue specimens were prepared – smooth, rectangular cross section specimens with no notch and notched specimens with three different notch severities.¹ The stress concentration factor (K_t) was 2.0 for the mild notch, 3.5 for the intermediate notch, and 5.0 for the sharp notch. The values of K_t were determined using information from Peterson.³

The smooth fatigue specimens were tested in both air and synthetic seawater, whereas the notched fatigue specimens were tested only in synthetic seawater. The synthetic seawater was prepared in accordance with the procedures given in ASTM Designation: D 1141 - 90. All testing was performed at room temperature (RT) using a 100-kN capacity closed-loop servo-hydraulic test system operated in load control. The axial loading was sinusoidal at a stress ratio of 0.1. The cyclic frequency was 10 Hz for tests in air and 1 Hz for tests in synthetic seawater. The specimens were cycled to failure or until they had been subjected to 1 million cycles without failure.

Many of the tests ‘ran out’ under certain test conditions; that is, they reached a large number of cycles without failure under those conditions. In those cases, the stress level was increased, and cycling was continued until the specimen failed or again ‘ran out.’ The fatigue lives shown in this paper indicate the number of cycles applied at the corresponding stress level; they are not cumulative values. After a ‘run out,’ the stress was increased by an amount large enough that the prior cycling was expected to have a negligible effect on fatigue life at the increased stress level. Three specimens failed at the grip end instead of within the test

section. Their fatigue lives are indicated to be greater than the number of cycles at which the grip end failed because there was no fatigue cracking in the test section.

For tests in synthetic seawater, the fatigue specimens were enclosed in a clear plastic test cell. A batch of synthetic seawater was prepared and poured into a plastic tank. The synthetic seawater was then slowly pumped through the test cell. The synthetic seawater leaving the test cell was drained into another tank and periodically discarded. Batches of fresh synthetic seawater were prepared several times a week, as needed. Thus, the test specimens were exposed to synthetic seawater that was continuously refreshed.

All of the fatigue specimens that were tested in synthetic seawater were cathodically polarized to either -0.90 V vs. the Ag/AgCl reference electrode or -1.13 V vs. the Ag/AgCl reference electrode. The level of -0.90 V vs. Ag/AgCl simulated adequate cathodic protection, while the level of -1.13 V vs. Ag/AgCl simulated cathodic overprotection. The specimens were polarized using a conventional, commercially manufactured laboratory potentiostat and platinum counter electrode.

All of the fatigue results are presented in Figure 1, which is a plot of the maximum nominal stress versus fatigue life. In cases where the specimen 'ran out' at more than one stress level before reaching a stress level where failure occurred, only the 'run-out' point immediately prior to the failure (i.e., the highest 'run-out' stress level) is plotted. The plus symbols are for the results of tests in air, while the other symbols are for the results of tests in synthetic seawater. The filled symbols represent specimens tested with adequate cathodic protection, while the open symbols represent specimens tested with cathodic overprotection.

The data in Figure 1 show that the fatigue strength decreased significantly as the notch severity increased, with the fatigue strength for $K_t = 5.0$ being about only one third of that for $K_t = 1.0$. The data for cathodic overprotection of smooth specimens (open circular symbols) fell slightly below the results of tests in air (plus symbols), whereas the data for tests with adequate cathodic protection (filled circular symbols) had fatigue strength above that in air. Notched specimens with adequate cathodic protection (filled symbols) also exhibited better fatigue strength than comparable specimens with cathodic overprotection (open symbols).

Fatigue Crack Growth

Three fatigue-crack-growth tests were performed in ASTM synthetic seawater at RT. The tests were performed in accordance with the procedures of ASTM Designation: E 647 - 95. Standard 25.4-mm wide by 12.7-mm thick CT specimens were machined from the ASTM A 710 steel plate, fatigue pre-cracked in air, and then tested in seawater. The synthetic seawater was prepared and circulated through a test cell that enclosed the CT specimen and test fixtures following the same procedures that were used in the S-N fatigue testing. One specimen was tested under free-corrosion conditions, one specimen was tested with a normal level of cathodic protection (-0.90 V vs. Ag/AgCl), and one specimen was tested with cathodic overprotection (-1.13 V vs. Ag/AgCl).

All fatigue-crack-growth testing was performed at room temperature (RT) using a closed-loop servo-hydraulic test system operated in load control. The applied load was cycled sinusoidally at a frequency of 1 Hz and a load ratio (R) of 0.1. These are the same frequency and load ratio that were used in the S-N fatigue testing. Crack length was measured by means of the DC electric potential drop method. The data were analyzed in accordance with the procedures of ASTM Designation: E 647 - 95 to produce cyclic crack growth rate (da/dN) values as a function of stress intensity factor range (ΔK).

The da/dN - ΔK data are presented in Figure 2 (open symbols) along with comparable data reported by Reynolds and Todd (filled symbols).⁴ For conditions of free corrosion and normal cathodic protection, the present results agree well with those of Reynolds and Todd.⁴ However, for cathodic overprotection (triangles), the present results fell well below those of Reynolds and Todd.⁴ This result is believed to be caused by crack closure and a resulting low effective stress intensity factor range in the current test with cathodic overprotection. During this test, a copious amount of calcareous scale formation was observed. The formation of such scale on the crack faces is postulated to reduce the effective stress intensity factor range markedly and in turn reduce the cyclic crack growth rate. Based on the results for conditions of free corrosion and normal cathodic protection, it was concluded that the ASTM A 710 steel used in the current study has corrosion-fatigue crack-growth behavior typical of that expected for this steel.

FATIGUE OF WELDED SPECIMENS IN SEAWATER

Steel marine structures are typically fabricated by welding various components together. The welds or base-metal regions adjacent to welds are the most likely locations for fatigue damage in marine structures that are subjected to cyclic loading. Thus, fatigue needs to be assessed in the design of these structures. For example, the API recommended practice for fixed offshore platforms⁵ provides procedures for assessing fatigue in the design of welded tubular connections.

Design methods for welded structures are based on the results of fatigue tests of specimens with welded joints. As reviewed by Jaske,⁶ Figure 3 illustrates configurations of welded joints that are commonly used for fatigue testing. Additionally, actual structural components such as tubular joints, built-up beams, piping connections, and pressure vessels are sometimes fatigue tested to develop data for realistic engineering equipment. These specimens and components have either full penetration welds or fillet welds. Either bending or axial cyclic loads are applied during fatigue testing. In some cases, pressure cycling is used in the fatigue testing.

The fatigue life of a welded joint consists of both a crack-initiation phase and a crack-propagation phase. Thus, total fatigue life depends on the relative contribution of each cracking phase and the definition of failure. Commonly used definitions of fatigue failure include initiation of a detectable crack, through-wall cracking, and total fracture. Total specimen fracture was the failure criterion for the S-N fatigue data shown in Figure 1. Since these were relatively long-life fatigue tests performed in load control, the specimens failed

rapidly once a significant crack (estimated to be 0.25 to 0.50 mm) developed. For this reason, the S-N curves provide a measure of the base metal's resistance to fatigue-crack initiation. Because both crack initiation and propagation can significantly contribute to the fatigue life of welded joints, so the experimental procedures for testing welded joints in this study were designed to detect crack initiation and measure crack growth.

Butt-welded and fillet-welded joints were selected for corrosion-fatigue testing. The specimens were loaded in three-point bending, as illustrated in Figures 4 and 5. The specimen and loading illustrated in Figure 4 correspond to Case 3 in Figure 3, while the specimen and loading illustrated in Figure 5 correspond to Case 8 in Figure 3. Bending was selected for the loading condition so that the specimens could be made from the full thickness (19 mm) of the ASTM A 710, Grade A, Class 3 steel plate.

Six butt-welded and six fillet-welded fatigue specimens were fabricated. Two pieces of plate were butt-welded to produce a joined plate; then, six specimens were cut from the welded assembly. Also, a 13.5-mm tee piece of plate was fillet welded to another plate; then, six specimens were cut from the welded assembly. Each specimen was 229 mm long by 63.5 mm wide by 19 mm thick, with a load span of 210 mm. Three levels of weld-toe severity were produced for each of the two types of specimens. The weld toes were ground, as-welded, or undercut. Thus, there were duplicate specimens for each combination of weld-toe severity and weld-joint type.

The welds were made using a 1.14-mm diameter flux-cored electrode as the filler. The wire designation was Lincoln Electrode Outershield⁽¹⁾ 91K2-H (classification AWS E91T1-K2MH8), and the shielding gas was C25 (75% Ar and 25% CO₂) at a flow rate of 0.85 m³/hr. Welding was performed in the flat position. The butt welds were made using backing bars on one side and 45-degree included angle weld preparation, with a 6.4-mm root opening. The travel speed was 0.33 to 0.36 m/min, the current was 210 to 220 A DCRP, and the voltage was 25 V. These welding parameters were upset in an effort to produce the samples with weld-toe undercut, but the desired defect could not be produced. Therefore, simulated undercut was produced using a sharp vee-shaped milling cutter. The simulated undercut was 1.42 to 1.52 mm deep with a 0.13 mm root radius.

Fatigue testing of the welded joints was performed at room temperature (RT) using a closed-loop servo-hydraulic test system operated in load control. The distance from each support pin to the central loading pin was 105 mm. The applied load was cycled sinusoidally at a frequency of 1 Hz and a load ratio (R) of 0.1. These are the same frequency and load ratio that were used in the S-N fatigue and fatigue-crack-growth testing. The refreshed, room-temperature synthetic seawater environment and cathodic polarization were maintained in the same manner as they were for the S-N fatigue and fatigue-crack-growth tests.

The DC electric potential drop method was used to detect crack initiation and measure crack growth. A constant current of 10 A was applied using a lead wire connected to each end

⁽¹⁾ Outershield 91K2-H is a trade name of the Lincoln Electric Company, Cleveland, Ohio.

of the specimen. These connections were centered on the mid-thickness and mid-width of the specimen. Lead wires for potential measurement were attached to the lower specimen surface adjacent to the toe of the weld. One lead wire was attached on one side of the weld joint near one edge of the specimen, while the other lead wire was attached on the other side of the weld joint near the other edge of the specimen. With this arrangement, the potential drop changes when cracking initiates on either side of the joint and gives a measure of average crack advance if the growth is non-uniform across the width of the specimen.

The cathodic polarization system was monitored throughout each test to make sure that reproducible levels of cathodic protection were obtained and maintained. The applied potential was controlled using potentiostat. The off potential was measured just after the applied potential was briefly interrupted. The difference between the on and off potential is the potential drop caused by the resistance of the seawater solution. The cathodic current density was calculated by dividing the cathodic current and by the exposed surface area of the specimen. The data indicated that cathodic protection was consistent from test to test.

The fatigue data for the welded joints are plotted in Figure 6. Based on the sensitivity of the potential drop measurements, initiation was estimated to correspond to the development of 0.25 to 0.50 mm deep crack at the weld toe. This crack size is similar to the estimate of significant crack size for S-N fatigue specimens, so the initiation fatigue life of the welded joints should be compared with those of the base-metal specimens. The open symbols indicate crack initiation, while the filled symbols indicate total failure. Values of maximum nominal bending stress (σ_{\max}) at the weld toe were calculated from the maximum applied load and the nominal specimen dimensions using elastic stress analysis.

Specimens with as-welded or ground weld toes had similar fatigue strengths. Grinding the weld toes usually caused a slight improvement in fatigue resistance. Specimens with undercut weld toes had very low fatigue strengths. The fatigue strength for adequate cathodic protection (see circles and triangles in Figure 6) was not significantly different than that for cathodic overprotection (see squares and diamonds in Figure 6). Butt welds (see circles and squares in Figure 6) had higher fatigue resistance than the fillet welds (see triangles and diamonds in Figure 6). The crack-initiation life ranged from 56 to 89 percent of the total life and was 69 percent of the total life on average.

The average change in crack length (Δa) was calculated using the Johnson⁷ equation based on the calibration of Schwalbe and Hellmann.⁸ Because of the noise in the potential drop measurements, a smoothing function was used in calculating values of da/dN as a function of ΔK . Once a smooth plot of Δa versus N was obtained, da/dN was computed by the secant method. The ratio of the loading span to thickness was $229/19 = 11$, so values of ΔK could be computed using Tada's solution⁹ for pure bending, as follows:

$$\Delta K = 3(S - 2x) \Delta P (\pi a)^{0.5} F(a/W) / (2BW^2) \quad (1)$$

where ΔP is load range, S is the load span, x is the distance from the mid-span to the weld toe, B is specimen width, W is the specimen thickness, and $F(a/W)$ is the following function:

$$F(a/W) = (2W \tan(\pi a / (2W)) / (\pi a))^{0.5} ((0.923 + 0.199(1 - \sin(\pi a / (2W)))^4) / \cos(\pi a / (2W))) \quad (2)$$

The term $(S - 2x)$ appears in Equation 1 because the fatigue cracking occurred at the toe of the weld and not at the mid-span of the specimen.

Figure 7 shows the fatigue-crack-growth data from the tests of the welded joints. The solid curve represents the trend to the data for CT specimens (see Figure 2). There is a large amount of scatter in the data, but the overall trend is similar to that obtained from the CT specimens. For adequate cathodic protection (filled and X symbols), the crack-growth data fell near the reference curve. For cathodic overprotection (open and + symbols), the crack-growth data fell below the reference curve. Thus, cathodic protection did not increase crack-growth rate, and it decreased the crack-growth rate significantly in some cases. The low crack-growth rates were most likely caused by calcareous scale in the crack reducing the effective value of ΔK , as explained previously in the discussion of fatigue crack growth behavior of the base metal.

Based on the results of this study, it was concluded that the fatigue life of welded joints can be modeled as a two-stage process – crack initiation followed by crack growth until final failure occurs. Crack initiation was defined as the development of a crack approximately 0.25 to 0.50 mm long. The crack initiation life can be described using S-N curves, while the crack growth life can be described using fracture mechanics. This approach is straightforward and should be applicable to other types of welded joints.

FATIGUE MODEL

The fatigue life of structural steel weldments can be modeled as a two-stage process made up of crack initiation and crack growth. If crack initiation is defined as the development of a crack approximately 0.25 to 0.50 mm long, fatigue crack initiation life can be described using S-N curves. Once the crack has reached this size, its growth can be characterized using fracture mechanics. Fatigue crack growth can be predicted by integrating the appropriate crack growth rate relationship. Then, total fatigue life is the sum of the crack initiation and growth lives.

Two approaches⁶ have been used to develop S-N fatigue data for weldments. One approach is to test different configurations of welded joints (see Figure 3) and develop an S-N curve for each type of joint. Then, in designing a welded structure, the engineer uses the S-N curve(s) for the type of joint(s) employed in the structure. This approach requires the development of large amount of fatigue test data and limits designs to the types of joints for which S-N curves are available. The other approach is to develop basic S-N curves for smooth or unnotched specimens of base metal and then to use fatigue-strength-reduction factors to predict the fatigue strengths of welded joints from the basic S-N data. The fatigue-strength-reduction factor (K_f) is the ratio of the fatigue strength of the smooth specimens to the fatigue strength of the welded specimens. The latter approach was applied in the current study.

As reviewed by Jaske,⁶ K_f may vary as a function of fatigue life and may depend both on stress concentration at a local discontinuity as well as local variations in material properties. For typical structural steel weldments, K_f is primarily a function of the local stress concentration and plasticity when fatigue life is based on crack initiation, and values of K_f can be estimated using K_t , the notch root radius (r), and a material parameter. The Peterson expression³ for K_f gave good results in the current study:

$$K_f = \frac{1}{(1 + \sqrt{a_N/r})} (K_t - 1) + 1 \quad (3)$$

where a_N is Neuber's constant. A value of $a_N = 0.163$ mm gave good correlations for the ASTM A 710, Grade A, Class 3 steel used in this research.

To compare the current results with those from past studies of ASTM A 710 steel conducted by Rajpathak and Hartt,^{10,11} the parameter $\Delta K/\sqrt{r}$ was also evaluated for the notched specimens. This parameter is only valid for notched specimens, so it cannot be used to correlate the data from tests of notched specimens with those from test of smooth specimens.

Figure 8 shows the fatigue data for the base-metal specimens plotted using the K_f times S_n local-stress parameter. Values of K_f were calculated using Equation 3. For each level of cathodic protection, the data were well correlated by the local stress computed using K_f . The data for specimens polarized to -1.13 V vs. Ag/AgCl (open symbols except inverted triangles) agreed well with those for specimens tested in air (inverted open triangles), while the data for specimens polarized to -0.90 V vs. Ag/AgCl (filled symbols) fell well above those for specimens tested in air (inverted open triangles). These results indicate that cathodic overprotection was somewhat detrimental compared with adequate cathodic protection, but neither level of cathodic protection gave worse fatigue resistance than specimens tested in air. The reference curve in Figure 8 represents the mean trend of the data for tests in air and in seawater at -1.13 V vs. Ag/AgCl.

Figure 9 compares the current fatigue results for notched specimens tested with cathodic overprotection (open symbols) with comparable fatigue data from the work of Rajpathak and Hartt^{10,11} (filled symbols). The latter work was performed using keyhole CT specimens. The keyhole had a 3.2 mm radius, and the local stress range (ΔS) was calculated as the value of $\Delta K/\sqrt{r}$. In that study, fatigue curves were developed for both free-corrosion and cathodic overprotection (-1.10 V vs. SCE) conditions, as is shown in Figure 9. For the current study, ΔS was computed using K_f and S_n ($\Delta S = 0.9 \times K_f \times S_n$), and ΔK was computed using the following expression for a double edge-notched specimen loaded in tension:¹²

$$K = (1.99 + 0.76 (a/W) - 8.48 (a/W)^2 + 27.36 (a/W)^3) S_n \sqrt{a} \quad (4)$$

The factor of 0.9 was used because the stress ratio for the current work was 0.1. The stress ratio for the other study was 0.5. Considering the difference in specimen configuration, stress

ratio, and the normal scatter in fatigue data, the current results were in good agreement with those of Rajpathak and Hartt.^{10,11}

Figure 10 shows the fatigue data for the weld-joint specimens plotted in terms of maximum local stress versus crack-initiation life. The reference curve for base-metal specimens (see Figure 8) is included for comparison with the weld-joint data. The reference curve provides a slightly conservative approximation of the weld-joint data, but the local stress approach with fatigue life based on crack initiation gives a reasonably good overall consolidation of the results for various weld-joint and weld-toe configurations that were evaluated.

The information presented in this paper shows that the local stress approach can be used to predict crack-initiation fatigue life (N_i) and that fracture mechanics can be used to predict crack-propagation fatigue life (N_p). Total fatigue life (N_f) is then equal to $N_i + N_p$. The value of N_i is obtained from reference S-N curve using K_f computed from Equation 3. The value of N_p is computed by integrating the relationship between ΔK and da/dN . This approach is a straightforward method that can be applied to the fatigue design of marine structures by engineers. Cathodic overprotection did not significantly degrade the fatigue behavior of the ASTM A 710, Grade A, Class 3 steel and welded joints, so the approach applies as long as an adequate level of cathodic protection is maintained.

CONCLUSIONS

The conclusions are based on the current corrosion-fatigue study of ASTM A 710, Grade A, Class 3 steel plate and welded joints made from this plate. The corrosive environment was ASTM synthetic seawater at room temperature. The loading was sinusoidal at 1 Hz and at a stress ratio of 0.1. Where comparisons could be made with published data from other corrosion-fatigue studies of ASTM A 710 steel in seawater, the current results were in good agreement with the published data. For this reason, the current results are believed to be representative of those expected for this steel.

When an adequate level of cathodic protection (-0.90 V vs. Ag/AgCl) was employed, the fatigue crack initiation resistance was slightly better than that in air, while the fatigue crack growth rate was about the same as that in air. Cathodic overprotection (-1.13 V vs. Ag/AgCl) degraded the fatigue crack initiation resistance slightly but did not reduce it below that in air. Cathodic overprotection reduced fatigue crack growth rate, probably by producing calcareous scale deposits within the crack that reduced the effective range of stress intensity factor.

The fatigue resistance of notched specimens with stress concentration factors of 2.0, 3.5, and 5.0 decreased as the stress concentration factor increased, and it was well correlated with that of unnotched specimens using the Peterson³ fatigue strength reduction factor to calculate local stress values at the notches. The fatigue strength reduction factor was determined using the stress concentration factor, a material parameter, and the notch root radius. The same fatigue strength reduction factor also gave good predictions of the fatigue crack initiation resistance of both butt-welded and fillet-welded joints.

The DC electric potential drop method was a good technique for detecting crack initiation and measuring crack growth in welded-joint specimens. The fatigue crack growth behavior of welded joints was well characterized using the standard fracture-mechanics approach. The crack growth data obtained from tests of welded joints agreed well with those from tests of standard fracture mechanics specimens.

The total fatigue life of welded joints can be predicted as the sum of the crack-initiation life and the crack-growth life. The crack-initiation life is obtained from a S-N curve using the local stress at the weld toe. The local stress is computed using the fatigue strength reduction factor. The crack-growth life is computed by integrating the crack-growth rate relationship.

ACKNOWLEDGEMENTS

The author acknowledges the support of Ship Structure Committee (SSC), under Contract DTICG23-92-C-E01002, for supporting this work. Mr. William Hanzalek of the American Bureau of Shipping chaired project advisory committee and Prof. William H. Hartt of Florida Atlantic University served as the technical advisor for that committee.

REFERENCES

1. C. E. Jaske, *Interactive Nature of Cathodic Polarization and Fatigue*, Report SSC-412, NTIS No. PB2000-108444, Ship Structure Committee, Washington, D.C., 2001.
2. C. E. Jaske, J. H. Payer, and V. S. Balint, *Corrosion Fatigue of Metals in Marine Environments*, MCIC Report 81-42, Springer-Verlag, New York and Battelle Press, Columbus, Ohio, 1981.
3. R. E. Peterson, *Stress Concentration Factors*, John Wiley & Sons, New York, 1974.
4. G. H. Reynolds, and J. A. Todd, *Threshold Corrosion Fatigue of Welded Shipbuilding Steels*, Report SSC-366, Ship Structure Committee, NTIS, Springfield, VA, 1992.
5. *Recommended Practice for Planning, Designing and Constructing Fixed Offshore Platforms*, API Recommended Practice 2A (RP 2A), American Petroleum Institute, Washington, D.C., 1991.
6. C. E. Jaske, "REPORT NO. 1: Interpretative Review of Weld Fatigue-Strength-Reduction and Stress-Concentration Factors," *Fatigue Strength Reduction and Stress Concentration Factors for Welds in Pressure Vessels and Piping*, Bulletin 432, Welding Research Council, Inc., New York, 1998.
7. H. H. Johnson, "Calibrating the Electric Potential Method for Studying Slow Crack Growth," *Materials Research & Standards*, Vol. 5, 1965, pp. 442-445.
8. K.-H. Schwalbe, and D. Hellmann, "Application of the Electrical Potential Method to Crack Length Measurements Using Johnson's Formula," *Journal of Testing and Evaluation*, Vol. 9, No. 3, 1981, pp. 218-221.

9. H. Tada, P. C. Paris, and G. R. Irwin, *The Stress Analysis of Cracks Handbook*, Second Edition, Paris Productions Incorporated, St. Louis, 1985.
10. S. S. Rajpathak, and W. H. Hartt, "Fatigue Crack Initiation of Selected High Strength Steels in Seawater," *Proceedings of the 7th International Conference on Offshore Mechanics and Arctic Engineering*, Vol. III, ASME International, New York, 1988, pp. 323-341.
11. S. S. Rajpathak, and W. H. Hartt, "Keyhole Compact Tension Specimen Fatigue of Selected High-Strength Steels in Seawater," *Environmentally Assisted Cracking: Science and Engineering*, ASTM STP 1049, American Society for Testing and Materials, West Conshohocken, PA, 1990, pp. 425-446.
12. D. Broek, 1978, *Elementary engineering fracture mechanics*, Second Edition, Sijthoff & Noordhoff, Alphen aan den Rijn, The Netherlands, 1978.

TABLE 1
CHEMICAL COMPOSITION OF ASTM A 710, GRADE A, CLASS 3 PLATE

Element	Specified Amount, %	Measured Amount, %
C	0.07 max.	0.07
Mn	0.40-0.70	0.57
P	0.025 max.	0.011
S	0.025 max.	0.002
Si	0.40 max.	0.34
Ni	0.70-1.00	0.95
Cr	0.60-0.90	0.68
Mo	0.15-0.25	0.22
Cu	1.00-1.30	1.07
Nb	0.02 min.	0.045
Sn	–	0.010
Al	–	0.024
V	–	0.003
Zr	–	0.000
Ti	–	0.002
B	–	0.0007
Ca	–	0.0017
Co	–	0.008
Pb	–	0.00
Fe	Balance	Balance

TABLE 2
TENSILE PROPERTIES OF ASTM A 710, GRADE A, CLASS 3 PLATE

Property	Specified Minimum Value	Measured Value
0.2% Offset Yield Strength, MPa (ksi)	515 (75)	640 (92.8)
Ultimate Strength, MPa (ksi)	585 (85)	697 (101)
Elongation in 2 inches, %	20	42

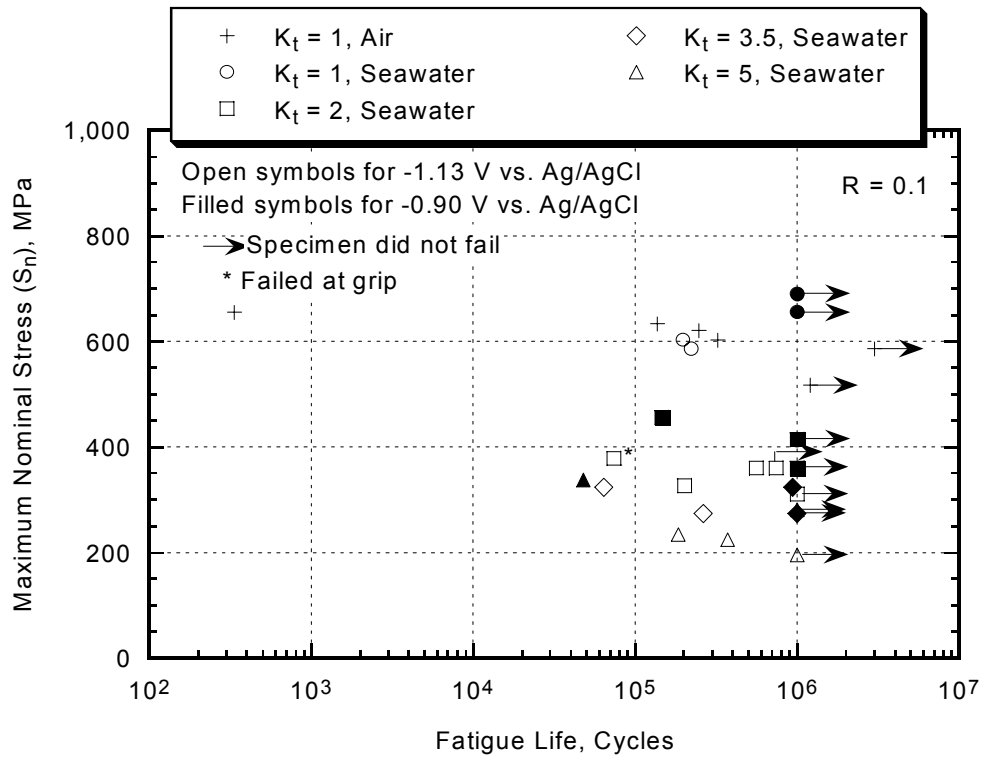


FIGURE 1 – Fatigue results for ASTM A 710, Grade A, Class 3 steel.

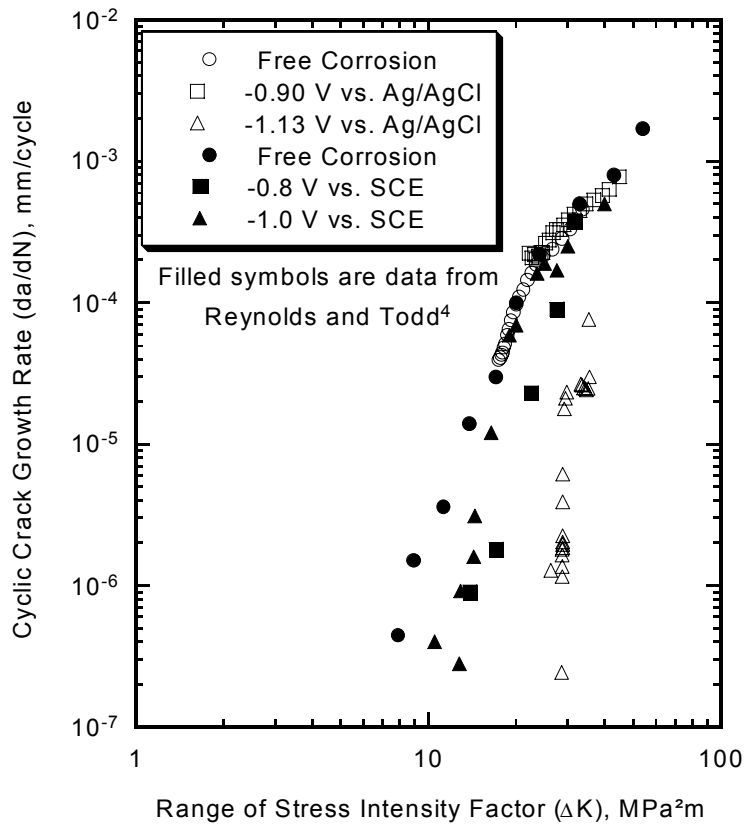


FIGURE 2 – Fatigue-crack-growth results for ASTM A 710, Grade A, Class 3 steel in synthetic seawater at room temperature.

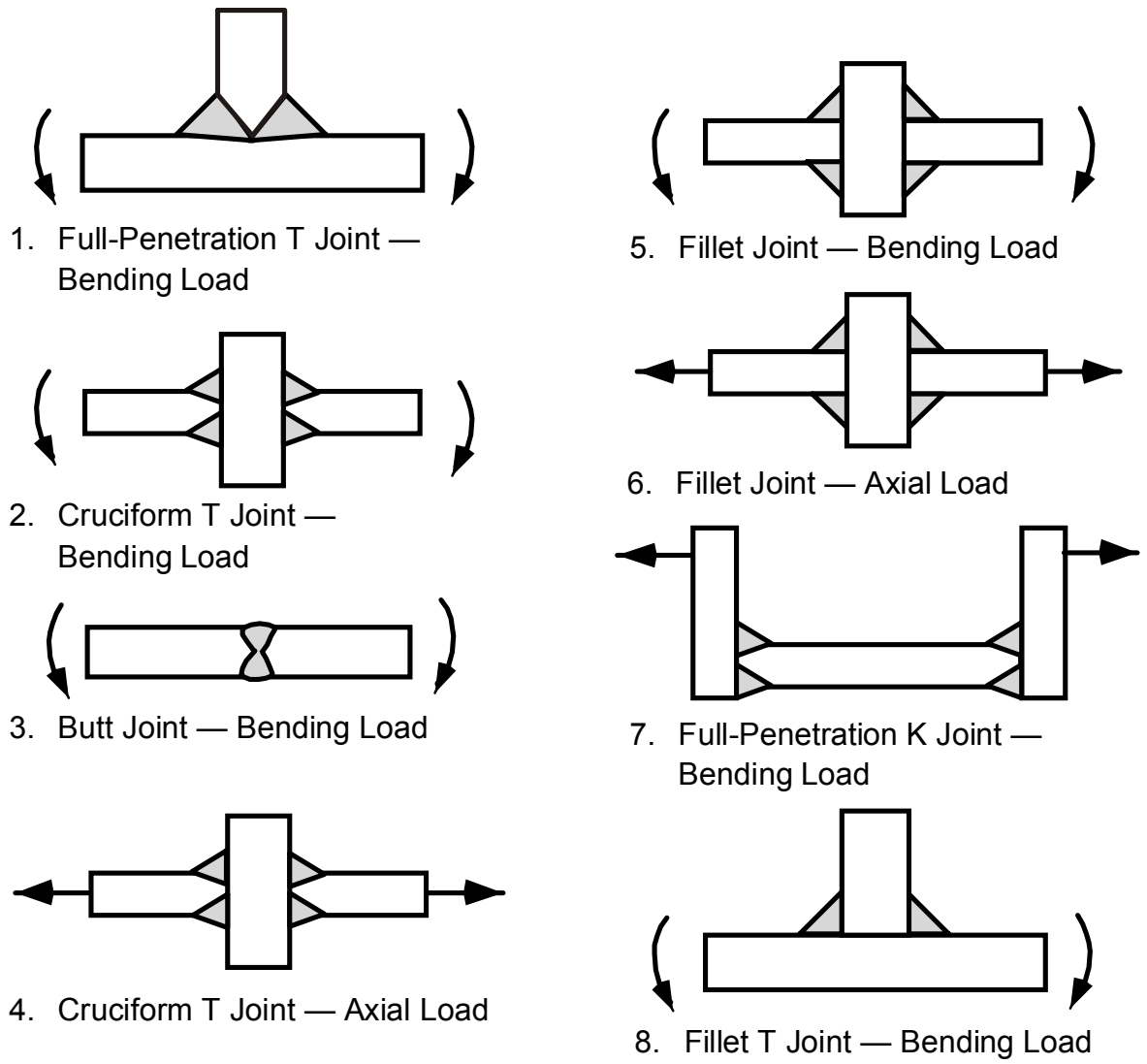


FIGURE 3 – Typical weld joints used for fatigue testing.⁶

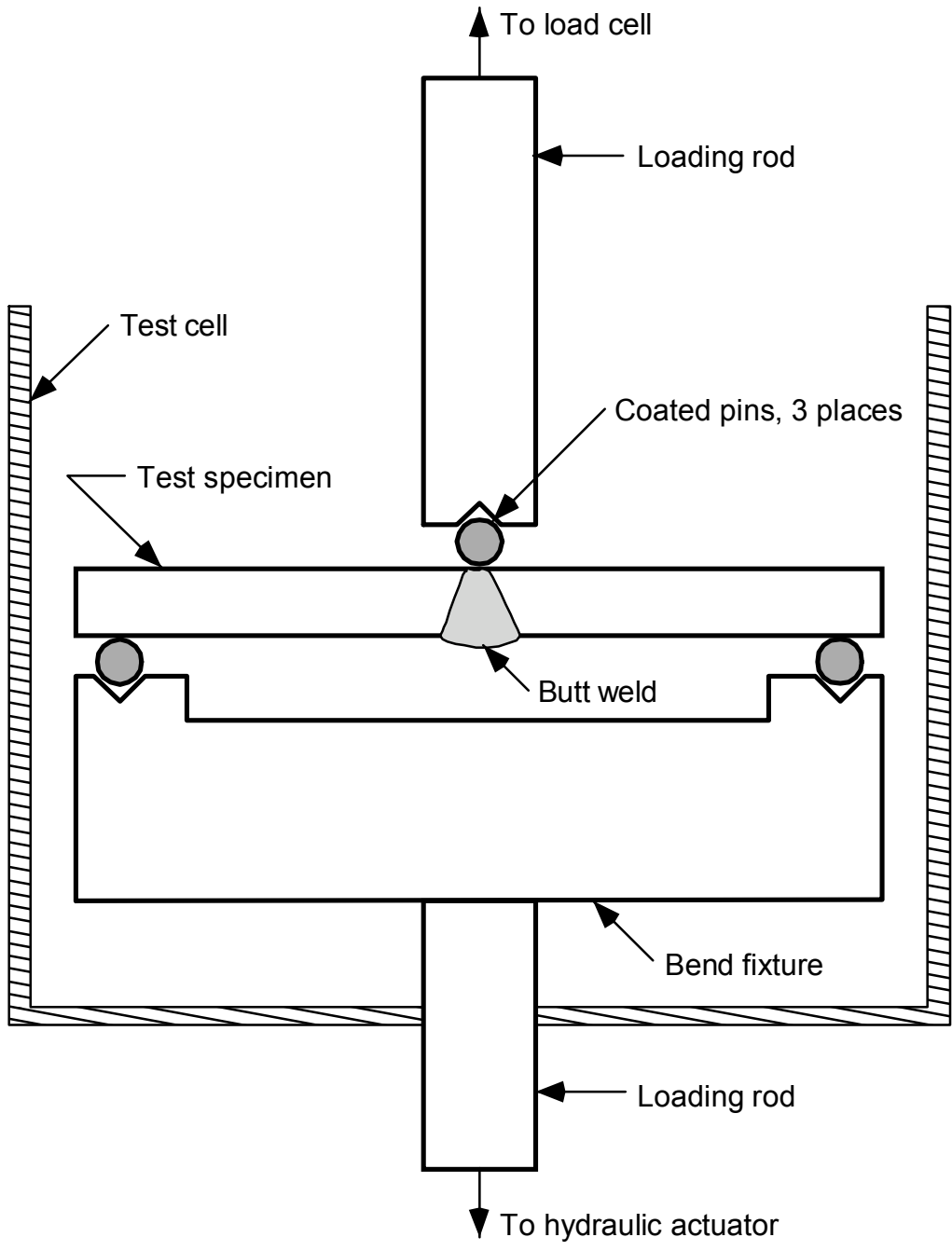


FIGURE 4 – Illustration of apparatus for fatigue testing of butt-welded joints.

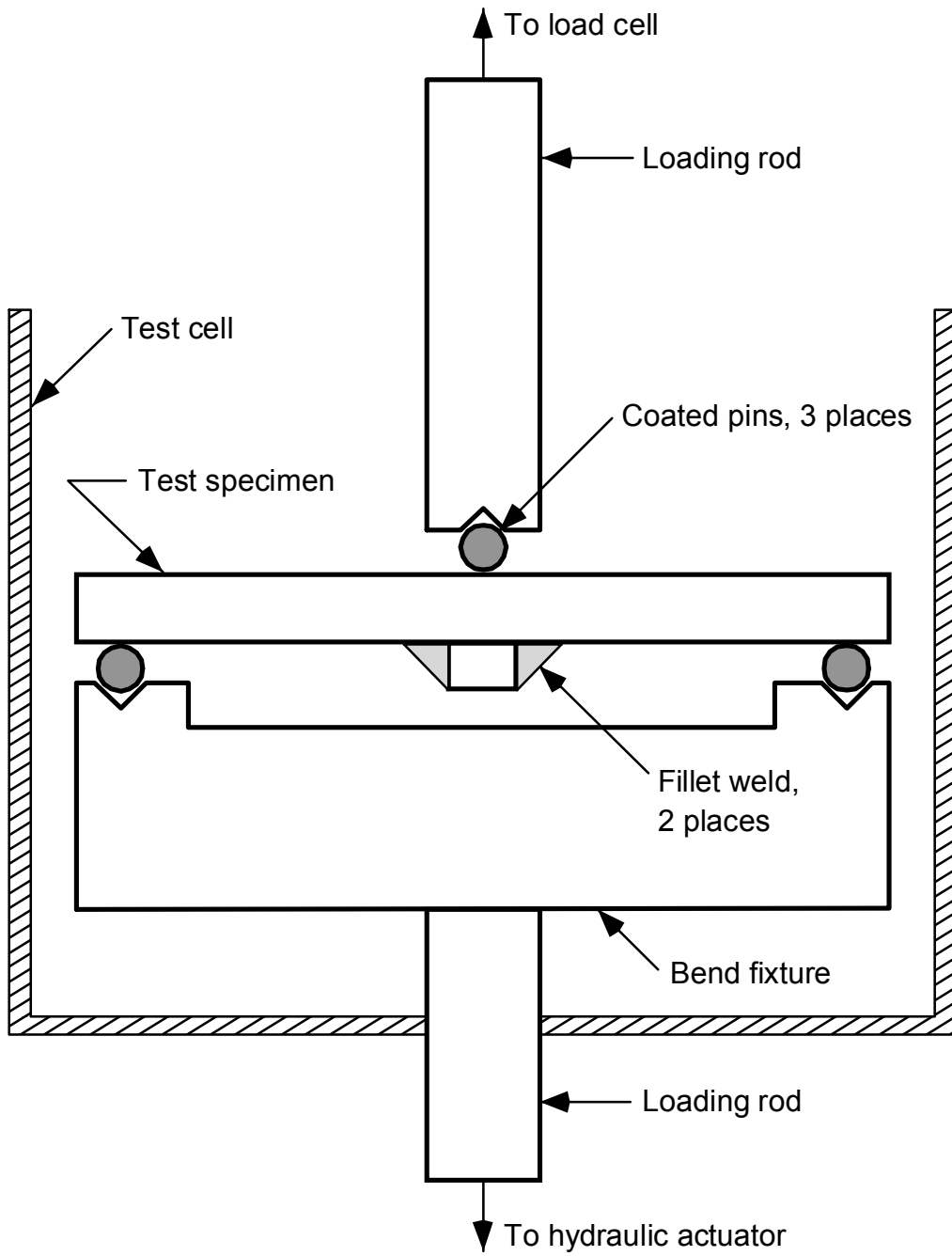


FIGURE 5 – Illustration of apparatus for fatigue testing of fillet-welded joints.

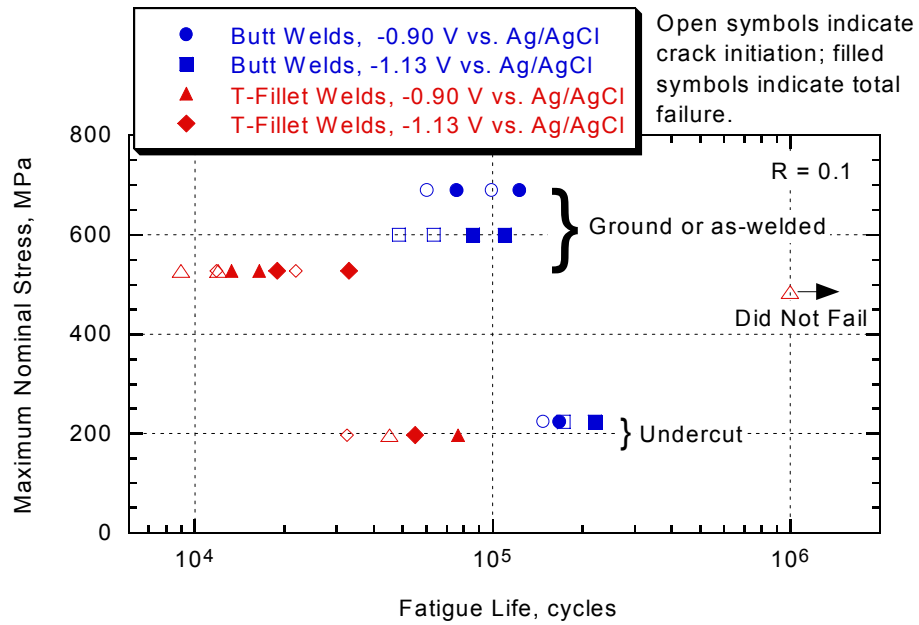


FIGURE 6 – Fatigue results for welded joints of ASTM A 710, Grade A, Class 3 steel in synthetic seawater at room temperature.

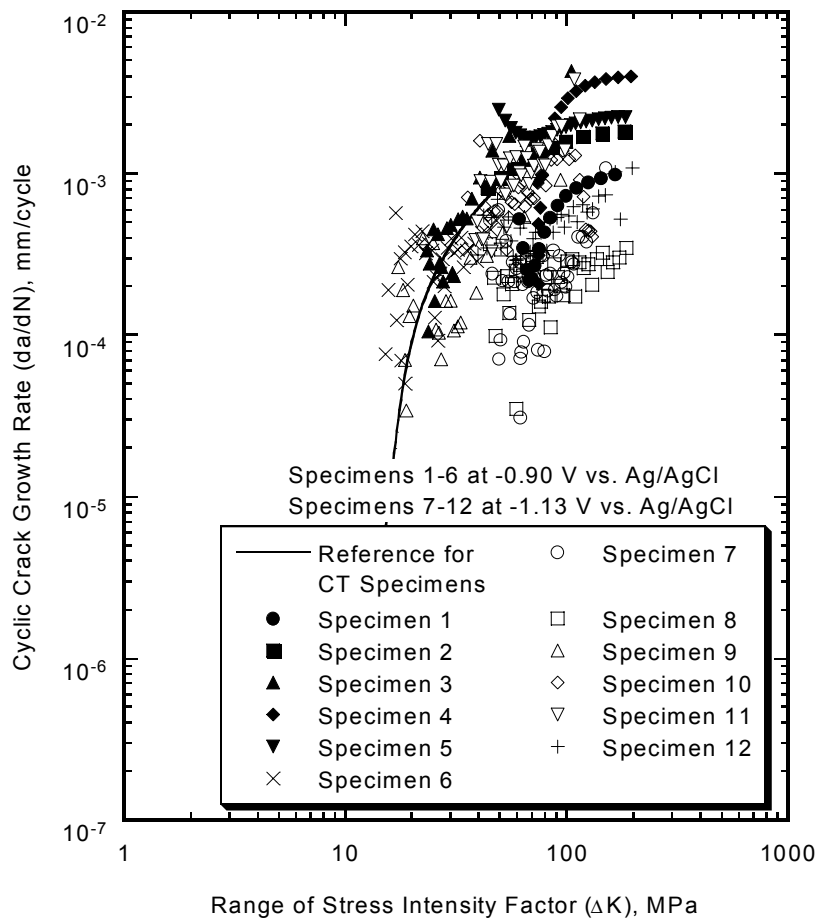


FIGURE 7 – Fatigue-crack-growth data from tests of welded joints of ASTM A 710, Grade A, Class 3 steel in synthetic seawater at room temperature.

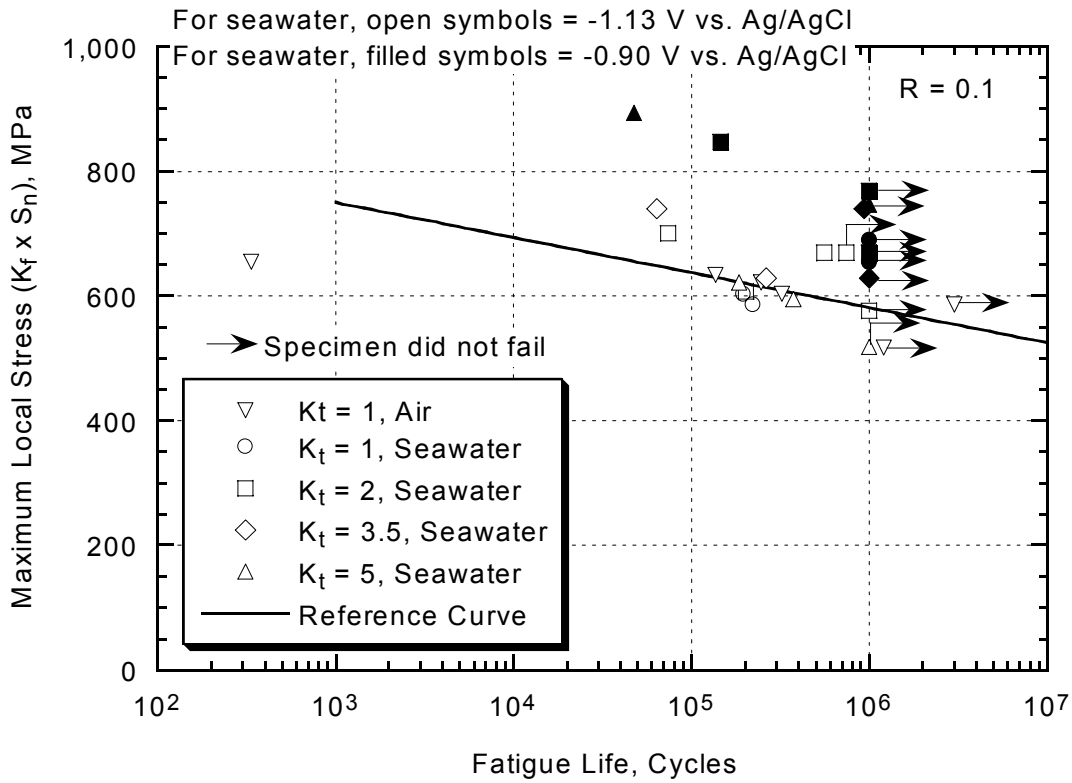


FIGURE 8 – Fatigue data for base-metal specimens as a function of maximum local stress.

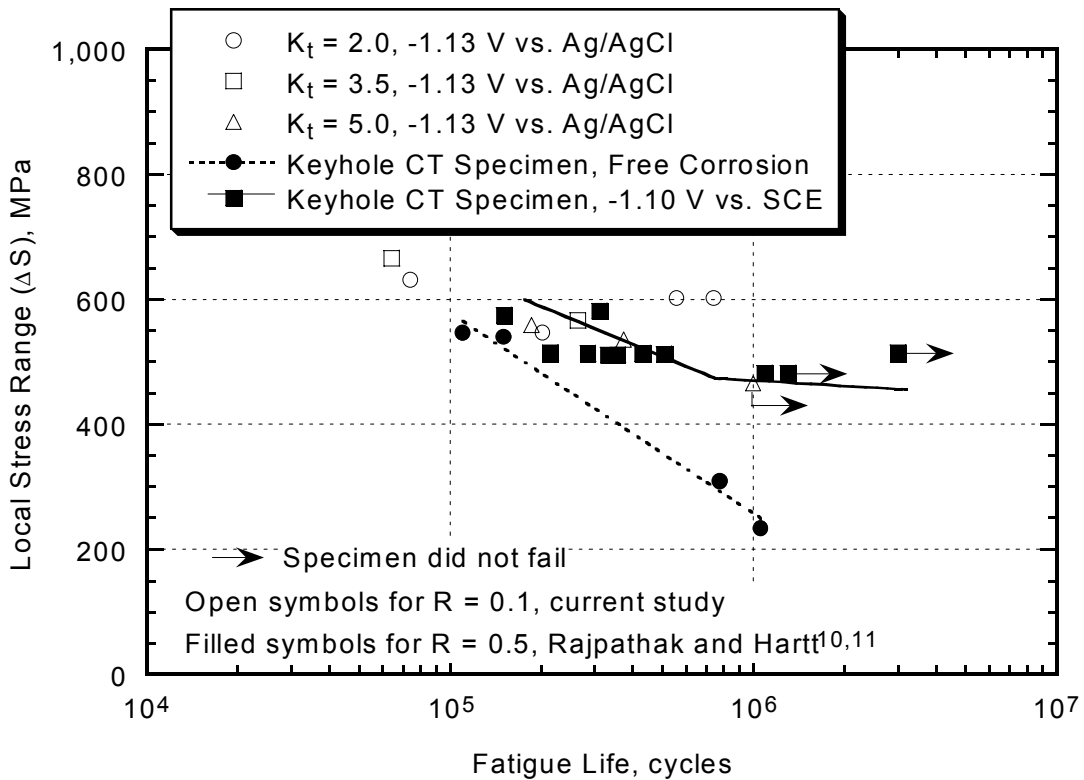


FIGURE 9 – Fatigue data for base-metal specimens as a function of local stress range.

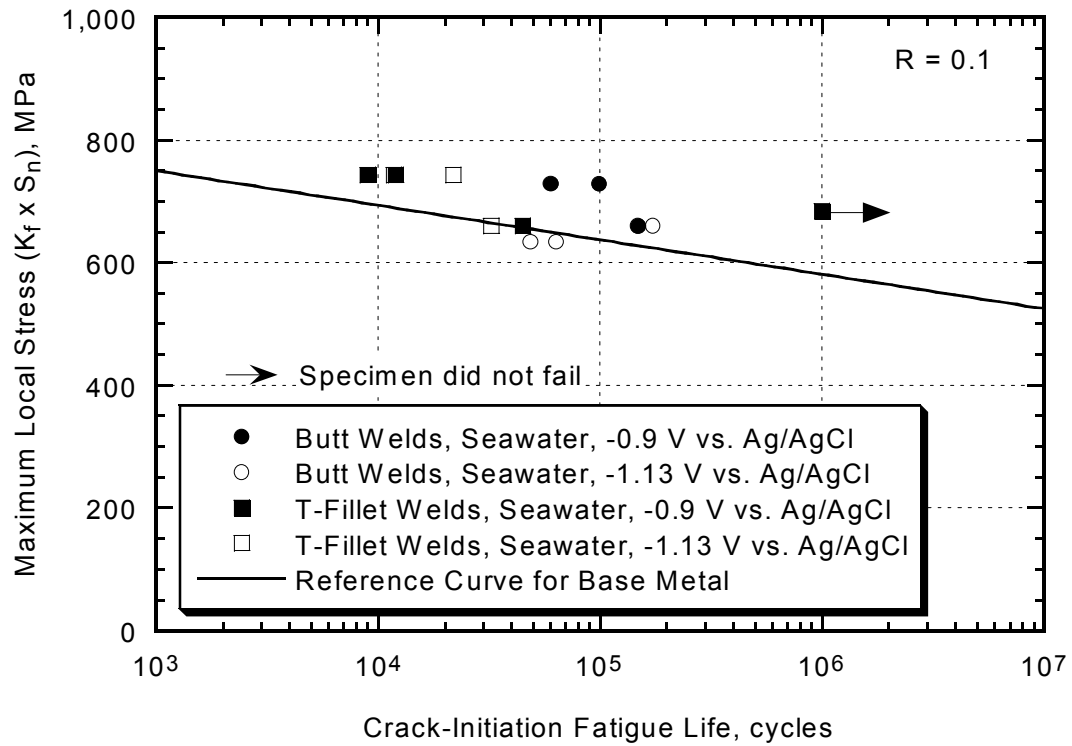


FIGURE 10 – Fatigue data for weld-joint specimens as a function of maximum local stress.